Supporting Information

Seed-mediated construction of bimetallic FeCo clusters on N-doped mesoporous carbon for bifunctional electrocatalysis in rechargeable Zn-air batteries

Yilun Zhao[a,c,d,e,#] Mengwei Duan[b,#], Zhengbin Tian[a,c,d*], Wenquan Wang[a,c,d,e], Xiaohui Deng[a,c,d], Bing Yu[b,*] and Guang-Hui Wang[c,c,d,e*]

[a] Qingdao Institute of Bioenergy and Bioprocess Technology, Chinese Academy of Sciences, Qingdao 266101, China

[b] College of Chemistry and Chemical Engineering, Institute of Biomedical Materials and Engineering, Qingdao University, Qingdao 266071, China

[c] Shandong Energy Institute, Qingdao 266101, China

[d] Qingdao New Energy Shandong Laboratory, Qingdao 266101, China

[e] University of Chinese Academy of Sciences, Beijing 100049, China

[#] These authors contribute equally to this work.

* Corresponding author. Email: wanggh@qibebt.ac.cn; yubing198@qdu.edu.cn; tianzb@qibebt.ac.cn.

Experimental section

Materials

All chemicals are of analytical grade and used without further purification. 3-aminophenol (3-AP) was obtained from J&K Chemicals Technology Co. Ltd. Pluronic® F127 (PEO_{106}-PPO_{70}-PEO_{106}) was purchased from Sigma-Aldrich (St. Louis, MO, USA). Co. Ltd (Shanghai, China). Oleic acid (OA), hexamethylenetetramine (HMT), $K_3[Co(CN)_6]$, and $K_3[Fe(CN)_6]$ were obtained from Sinopharm Chemical Reagent. Co. Ltd (Shanghai, China). The commercial Pt/C (20%) catalyst was obtained from Johnson Matthey. The commercial RuO_2 (20%) catalyst was obtained from Macklin Biochemical Co. Ltd (Shanghai, China). The Nafion solution (5 wt%) was obtained from DuPont.

Materials characterization

The morphology of samples was examined by ZEISS GeminiSEM 360 microscope (SEM) and Hitachi-7650 transmission electron microscope (TEM) with an acceleration voltage of 10 kV and 100 kV, respectively. High-resolution transmission electron microscope (HRTEM) images, high-angle annular dark field scanning transmission electron microscope (HAADF-STEM) images and elemental mapping images were recorded on FEI Talos F200S instrument at an acceleration voltage of 200 kV. X-ray diffraction (XRD) patterns were measured at room temperature using a Bruker D8 Advance X-ray diffractometer at 40 kV and 40 mA with Cu K_α radiation (k = 1.5406 Å). X-ray photoelectron spectroscopy (XPS) measurements were conducted on a Thermo Scientific K-Alpha using Al Kα ($h\nu$ = 1486.6 eV) radiation equipped with 500 μm X-ray spot at 3×10^{-10} mbar and all the binding energy data were calibrated by C 1s (284.6 eV). The peak fitting was analyzed using XPSPeak software with Shirley-type background and Lorentzian-Gaussian shapes and signals were referenced by Handbook of Monochromatic XPS Spectra. The metal contents of the samples were determined using an inductively coupled plasma-optical emission spectrophotometer (ICP-OES; Agilent 5110, USA). Nitrogen content was analyzed using a Vario EL cube elemental analyzer (Elementar, Germany). Nitrogen sorption isotherms were measured with a Micromeritics ASAP 2460 instrument at 77 K. Prior to the measurements, the sample was degassed at 200 °C for 6 h. The specific surface areas and pore size distribution curves were calculated from the adsorption branch.

Electrochemical measurements

The electrochemical measurements were performed using a three-electrode system with a graphite electrode as the counter electrode, Ag/AgCl (saturated KCl solution) as the reference electrode, a rotating disk electrode (RDE) made of glassy carbon (GC, 4 mm in diameter) coated with the sample as the working electrode and an aqueous O_2-saturated 0.1 M KOH solution for ORR or Ar-saturated 1 M KOH for OER as the electrolyte. All potentials were reported versus the standard reversible hydrogen electrode (RHE). The working electrodes were prepared as follows: 10 mg of sample was ultrasonically dispersed in 975 μL of ethanol and 25 μL of Nafion solution to obtain a homogeneous ink. Afterward, 5 μL of the prepared catalyst ink (0.05 mg) was dropped on the polished electrode surface to achieve catalyst loadings of 0.4 mg cm^{-2} for ORR and 0.7 mg cm^{-2} for OER.

Linear sweep voltammetry (LSV) was performed with a scan rate of 10 mV s^{-1} (5 mV s^{-1} for OER) with 1600 rpm rotation speeds at room temperature for ORR. The ORR stability of the electrocatalysts was examined by accelerated deterioration tests (ADT) with a scan rate of 50 mV s^{-1} for 5,000 cycles between 0.6 and 1.0 V (vs RHE). The electrochemical impedance spectroscopy data were collected for the electrodes at the half wave potential ($E_{1/2}$).

Rotating ring-disk electrode (RRDE) measurements were conducted to investigate the H_2O_2 yield and the electron transfer number (n). The RRDE electrode was scanned at 10 mV s^{-1} with the ring potential being kept at 1.25 V (vs RHE). The H_2O_2 yield (H_2O_2%) and n were calculated by the following equations:

$$H_2O_2\% = 200 \times \frac{\frac{I_r}{N}}{\frac{I_r}{N} + I_d}$$

$$n = 4 \times \frac{I_d}{\frac{I_r}{N} + I_d}$$

where I_d is the disk current, I_r is the ring current, and $N = 0.37$ is the current collection efficiency of the Pt ring.

Re-ZABs Assembly and Measurements

The homemade Re-ZABs were assembled by using polished zinc foil (30 and 150 μm) as the anode and aqueous solution containing 6 M KOH with 0.2 M zinc acetate as the electrolyte. The as-prepared catalysts or commercial coated on carbon paper were used as the air cathode. The loading amount of the catalysts on carbon paper was 1.5 mg/cm^2 for both as-prepared catalysts and commercial catalysts. The discharge/charge polarization curves were measured using CHI 760E. For the cycling stability test, the Re-ZABs based on FeCo/SMC and Pt/C with RuO_2 (with a mass ratio of 1:1) were assembled. The galvanostatic discharge/charge cycling stability for ZABs was measured using a LANE (CT3002A) instrument with 15 min for discharging and 15 min for charging under ambient conditions.

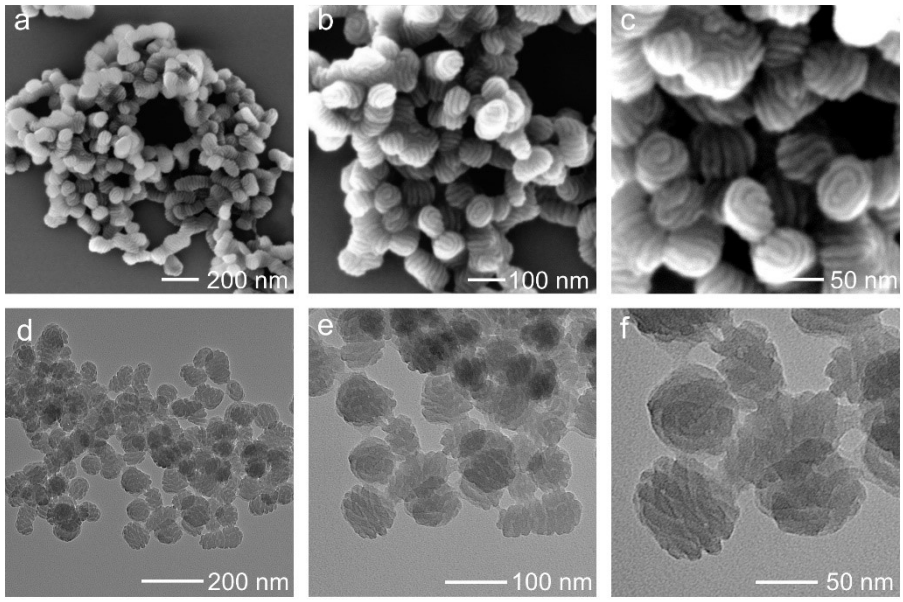

Fig. S1. (a-c) SEM and (d-f) TEM images of SMP.

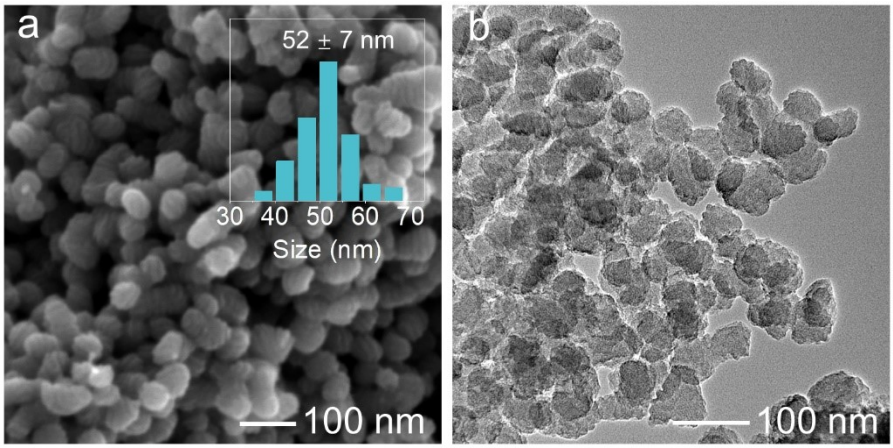

Fig. S2. (a) SEM and (b) TEM images of FeCo/SMC (inset in a is the size distribution of SMC).

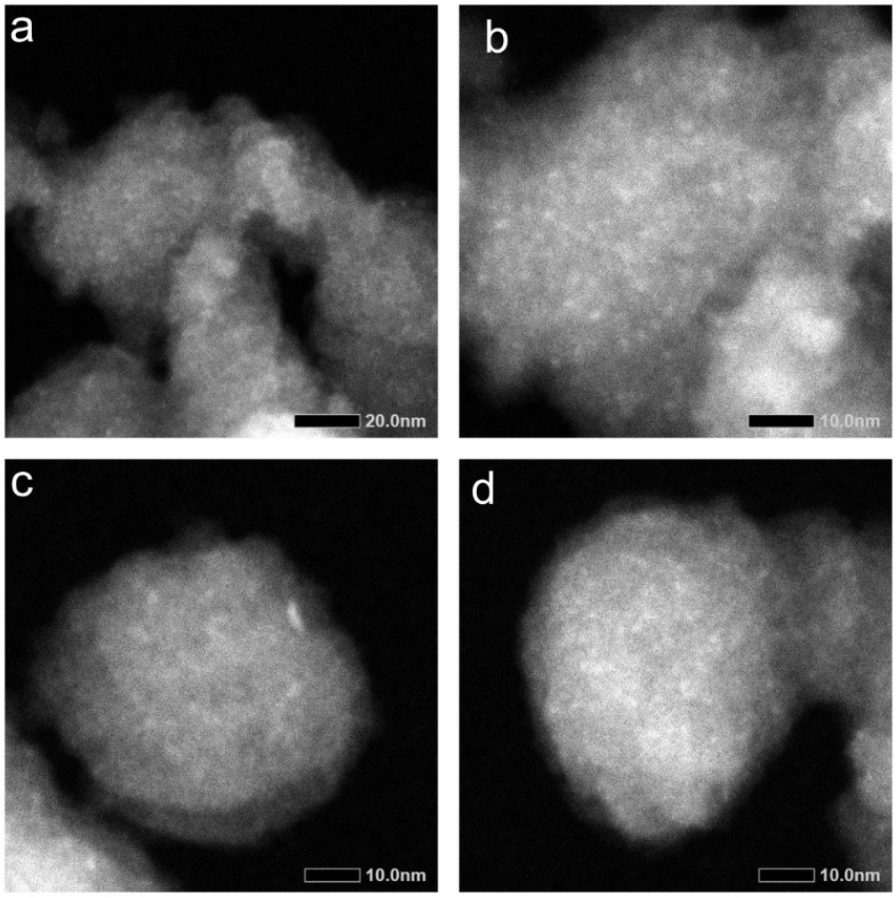

Fig. S3. HAADF-STEM images of FeCo/SMC.

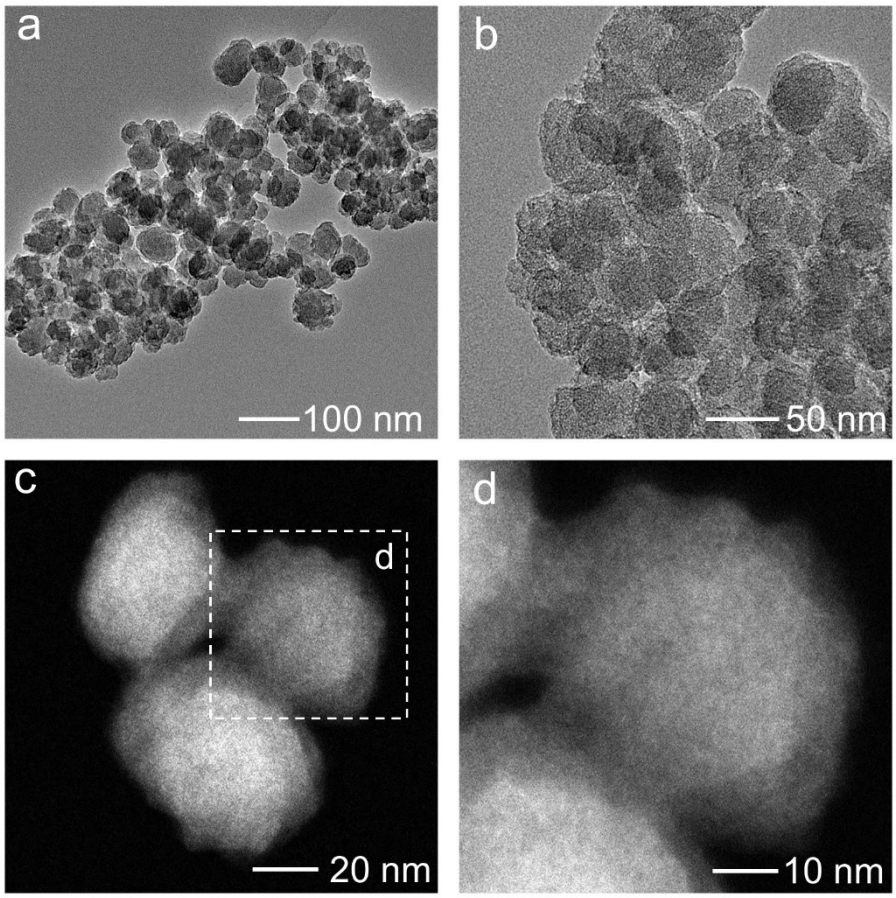

Fig. S4. (a,b) TEM and (c,d) HAADF-STEM images of Co_1/SMC.

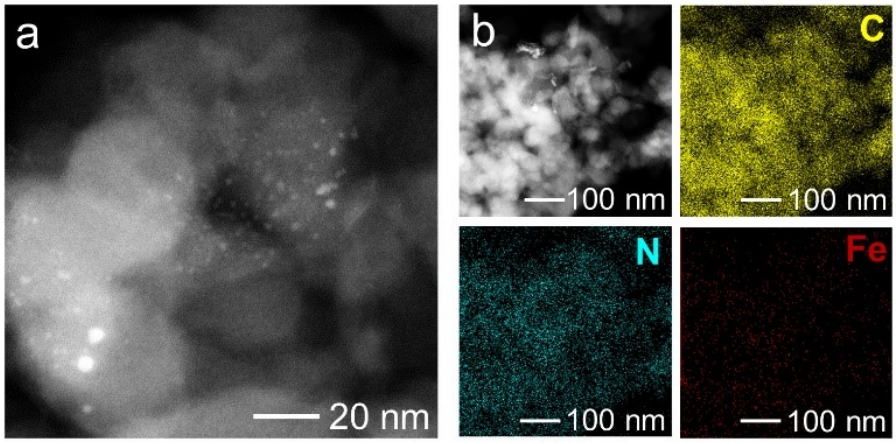

Fig. S5. HAADF-STEM and EDX elemental images of Fe-NPs/SMC.

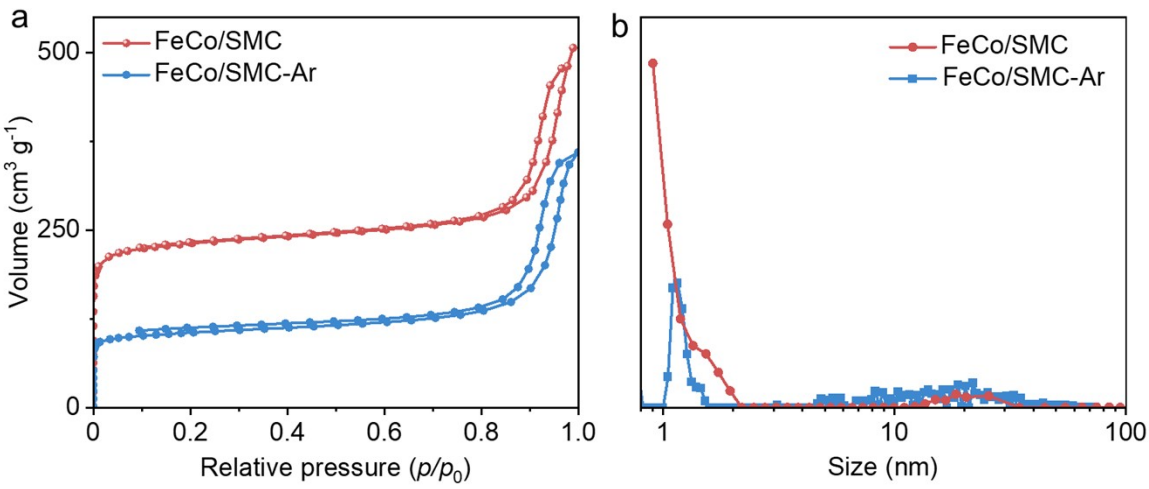

Fig. S6. (a) N_2 sorption isotherms and (b) pore size distributions of FeCo/SMC and FeCo/SMC-Ar.

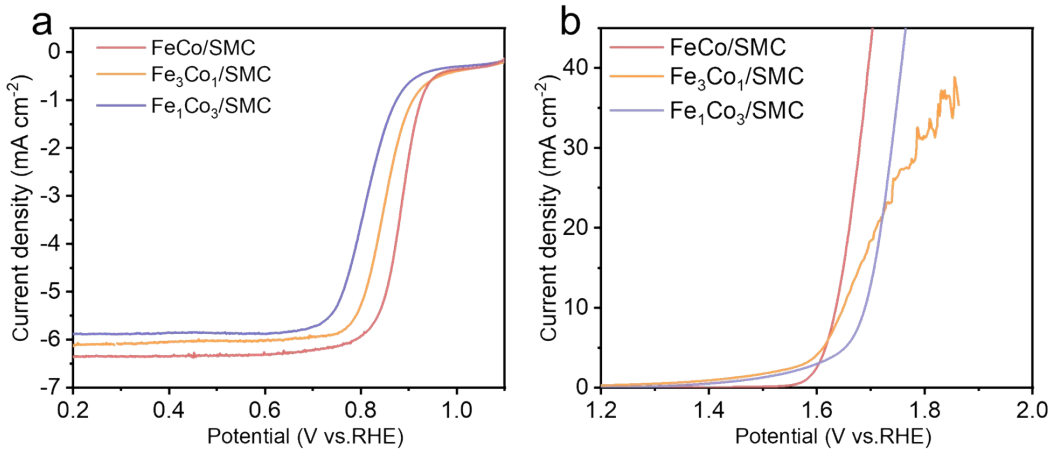

Fig. S7. ORR LSV curves and (b) OER LSV curves of Fe_1Co_3/SMC, Fe_3Co_1/SMC and FeCo/SMC.

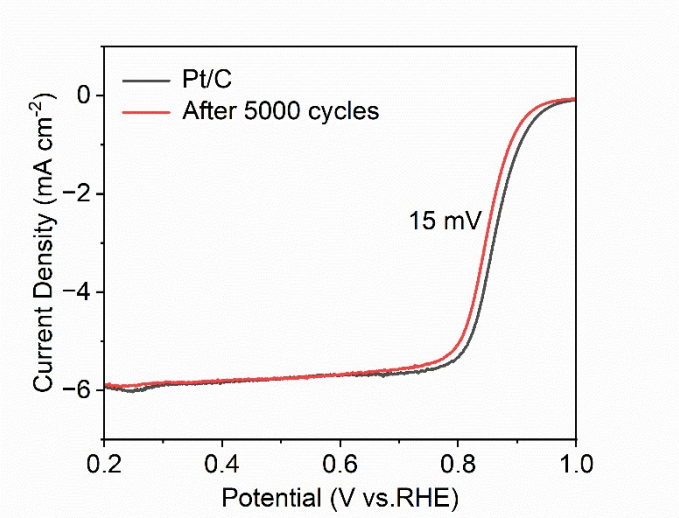

Fig. S8. ORR LSV curves of Pt/C before and after 5000 cycles.

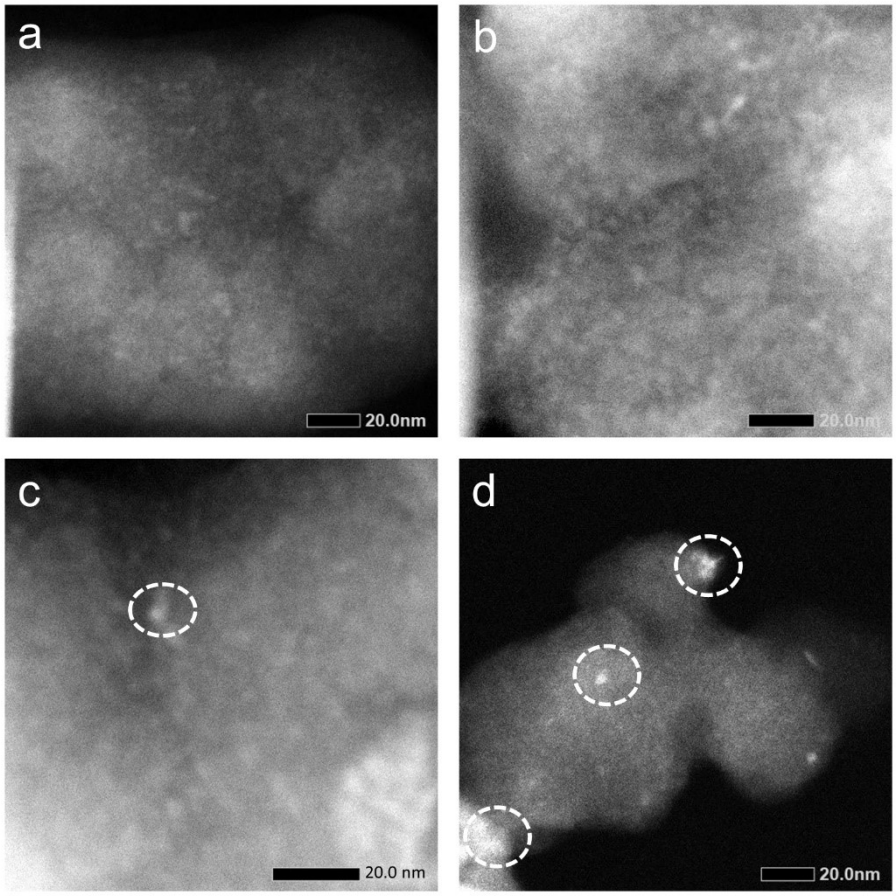

Fig. S9. HAADF-STEM images of FeCo/SMC after use.

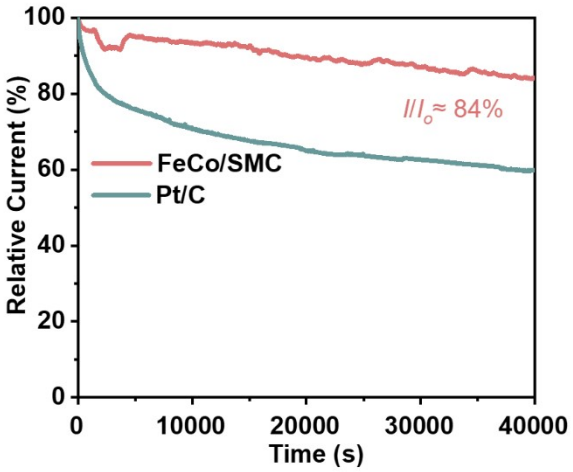

Fig. S10. Chronoamperometry curves of FeCo/SMC and Pt/C at 0.7 V vs RHE.

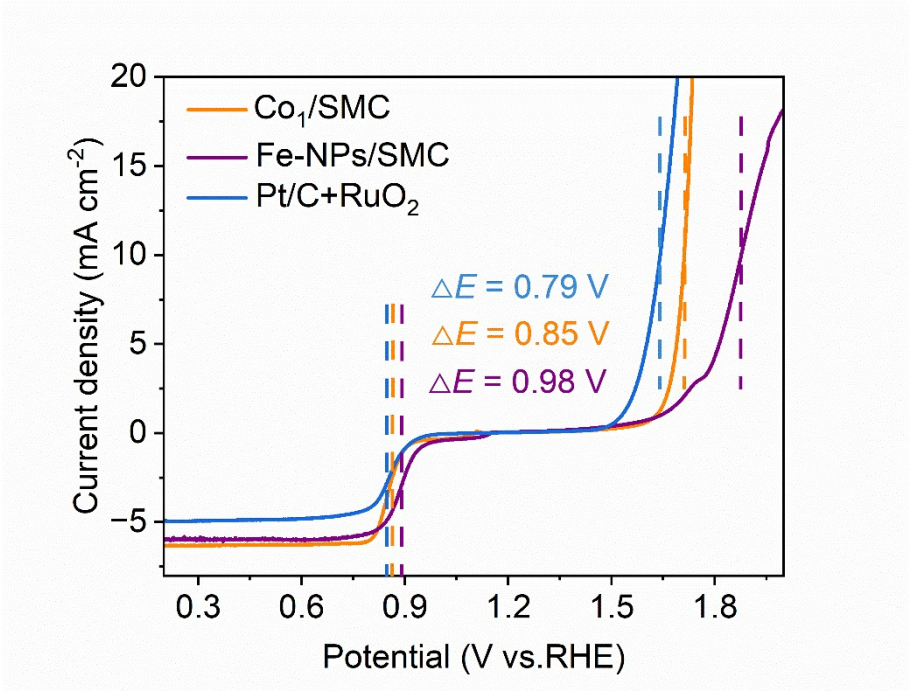

Fig. S11. ΔE value of Co_1/SMC, Fe-NPs/SMC and Pt/C+RuO_2.

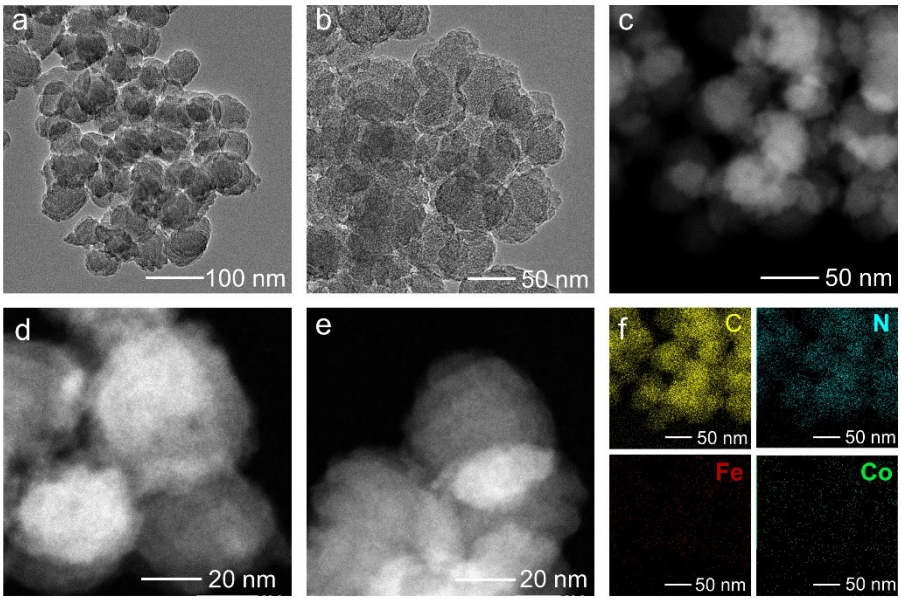

Fig. S12. (a,b) TEM images, (c-e) HAADF-STEM images and (f) corresponding EDX elemental images of FeCo/SMC-Ar.

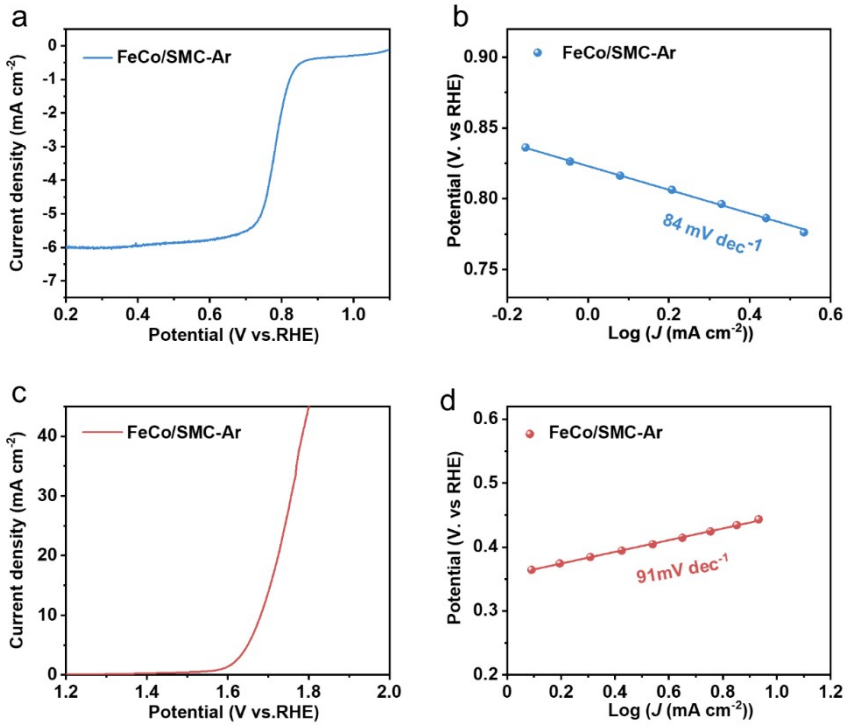

Fig. S13. (a) ORR LSV polarization curve and (b) Tafel slope of FeCo/SMC-Ar, (c) OER LSV polarization curve and (d) Tafel slope of FeCo/SMC-Ar.

Table S1. Textural parameters and chemical composition of FeCo/SMC and FeCo/SMC-Ar.

Sample	Textual properties		Chemical composition		
	S_{BET} (m^2/g)	V_{total} (cm^3/g)	C wt%	N wt%	H wt%
FeCo/SMC	897	0.78	80.8	9.0	2.0
FeCo/SMC-Ar	412	0.54	79.7	7.3	2.1

Table S2 Summary of bifunctional activities of carbon supported transition metal-based catalysts.

No.	Catalysts	$E_{1/2}$ (V vs RHE)	$E_{j=10}$ (V vs RHE)	ΔE ($E_{j=10}$-$E_{1/2}$) (V vs RHE)	Reference
1	**FeCo/SMC**	**0.89**	**1.609**	**0.72**	**This work**
2	Co_3Fe_7/NC	0.85	1.59	0.74	*Carbon Energy*, **2025**, *7*, e682
3	Ag/Co/Co_3O_4@NC	0.853	1.563	0.71	*ChemPhysChem* **2025**, *26*, e202500496
4	Fe_{800}-HZIF8	0.84	1.527	0.687	*J. Energy Storage* **2025**, *137* 118723
5	P/Co-N-C-2	0.80	1.668	0.86	*J. Alloy. Compd.* **2025**, *1040*, 183507
6	FeCo/NC-7	0.92	1.580	0.66	*J. Power Sources* **2025**, *644*, 236996
7	A-Co-Fe/NCF-CoNP	0.89	1.58	0.69	Small **2025**, *21*, e06084
8	FeCo-NBC	0.88	1.534	0.66	*ACS Sustainable Chem. Eng.* **2025**, *13*, 13979
9	CoFe@NC-5	0.84	1.597	0.757	*Phys. Chem. Chem. Phys.* **2025**, *27*, 14504
10	CoFe-Co_xN@NOALC	0.82	1.702	0.882	*Chinese Chem. Lett.* **2025**, *36*, 110403
11	Fe–N–C/Gra-600	0.862	1.743 V	0.881	ChemCatChem **2025**, *17*, e00731
12	Co-NSP-HPC	0.898	1.590	0.69	*Appl. Catal. B-Environ. Energy* **2025**, *365*, 124889
13	(Fe_3C, Fe_3P)/NC	0.85	1.727	0.88	*ACS Appl. Energy Mater.* **2025**, *8*, 529
14	CoNi-NCNT	0.81	1.52	0.71	*J. Colloid Interf. Sci.* **2025**, *683*, 631
15	B-Co/$CoSe_2$@NSeC	0.865	1.600	0.735	*Appl. Catal. B-Environ. Energy* **2025**, *362,* 124725
16	MPFeNi@NC-900	0.895	1.613	0.718	*J. Energy Storage* **2025**, *105*, 114740
17	FeN_4/MoO_x	0.902	1.567	0.665	*Adv. Funct. Mater.* **2025**, *35*, 2416215
18	P-FeNi-NPC	0.845	1.55	0.705	*Small* **2025**, *21*, 2402762
19	Co_3S_4@NCNT/NCHS	0.80	1.46	0.66	*J. Alloy*. *Compd*. **2024,** *1008*, 176679
20	CoFe-FeNC	0.876	1.526	0.65	*Appl. Catal. B-Environ. Energy* **2024**, *359*, 124485
21	$FeCo_5$-NC	0.908	1.670	0.762	*Electroanal. Chem.* **2024**, *965*, 118369
22	FeMn-N/S-C-1000	0.924	1.617	0.693	*J. Energy Chem.* **2024**, *90*, 610

Table S2 (contd.)

No.	Catalysts	$E_{1/2}$ (V vs RHE)	$E_{j=10}$ (V vs RHE)	ΔE ($E_{j=10}$-$E_{1/2}$) (V vs RHE)	Reference
23	FeCo/N-CF	0.886	1.672	0.786	*J. Energy Chem.* **2023**, *76*, 470
24	$Co_{14}Fe_1$-CNTF	0.82	1.480	0.66	*Adv. Mater. Interfaces* **2023**, *10*, 2201817
25		0.925	1.623	0.698	*Angew. Chem. Int. Ed.* **2023**, *62*, e202219191
26	CoP_3/-CeO_2/C-2	0.752	1.569	0.817	*Appl. Catal. B-Environ.* **2023**, *321,* 122029
27	CoNi@NCNTs/CC	0.82	1.56	0.74	Appl. *Catal. B-Environ.* **2022**, *317*, 121764
28	NiFe@C@Co CNFs	0.87	1.600	0.73	Small **2022**, *18*, 2200578
29	3D Co/N-C	0.84	1.56	0.72	*Chem. Eng. J.* **2022**, *433*, 134500
30	Co-N-CCNFMs	0.84	1.559	0.719	*Energy Storage Mater.* **2022**, *47*, 365
31	Fe-Mo-N-C/800	0.856	1.66	0.804	*Chem. Eng. J.* **2022**, *449*, 137705
32	FeCo−NC	0.877	1.579	0.702	*ACS Catal.* **2022**, *12*, 1216
33	Co-CoN_4@NCNs	0.83	1.54	0.71	Adv. *Funct. Mater.* **2022**, *32*, 2207331
34	D-Co@NC	0.852	1.718	0.866	*Chem. Eng. J.* **2022***, 431,* 133734
35	FeCo-1/NSC	0.82	1.555	0.735	*J. Energy Chem.* **2021**, *56*, 64
36	FeNi/N−LCN	0.835	1.57	0.735	*Nano Lett.* **2021**, *21*, 3098
37	FeNi/N−C-900	0.81	1.643	0.833	*Chem Asian J.* **2021**, *16*, 1592